Journal of Materials Chemistry A

# Reducing sputter induced stress and damage for efficient perovskite/silicon tandem solar cells

| | |
|---|---|
| Journal: | *Journal of Materials Chemistry A* |
| Manuscript ID | TA-ART-10-2021-009143.R1 |
| Article Type: | Paper |
| Date Submitted by the Author: | 10-Dec-2021 |
| Complete List of Authors: | Liu, Kong; Institute of Semiconductors, Chinese Academy of Sciences, Key Laboratory of Semiconductor Materials Science<br>Chen, Bo; The University of North Carolina at Chapel Hill, Department of Applied Physical Sciences<br>Yu, Zhengshan; Arizona State University, School of Electrical, Computer, and Energy Engineering<br>Wu, Yulin; Institute of Semiconductors, Chinese Academy of Sciences, Key Laboratory of Semiconductor Materials Science<br>Huang, Zhitao; Institute of Semiconductors, Chinese Academy of Sciences, Key Laboratory of Semiconductor Materials Science<br>Jia, Xiaohao; Institute of Semiconductors, Chinese Academy of Sciences, Key Laboratory of Semiconductor Materials Science<br>Li, Chao; Institute of Semiconductors, Chinese Academy of Sciences, Key Laboratory of Semiconductor Materials Science<br>Spronk, Derrek; The University of North Carolina at Chapel Hill, Department of Applied Physical Sciences<br>Wang, Zhijie; Institute of Semiconductors, Chinese Academy of Sciences, Key Laboratory of Semiconductor Materials Science<br>Wang, Zhanguo; Institute of Semiconductors, Chinese Academy of Sciences, Key Laboratory of Semiconductor Materials Science<br>Qu, Shengchun; Institute of Semiconductors, Chinese Academy of Sciences, Key Laboratory of Semiconductor Materials Science<br>Holman, Zachary; Arizona State University, School of Electrical, Computer, and Energy Engineering<br>Huang, Jinsong; University of North Carolina at Chapel Hill, Department of Applied Physical Sciences; University of Nebraska-Lincoln, Department of Mechanical and Materials Engineering |
| | |

ARTICLE

# Reducing sputter induced stress and damage for efficient perovskite/silicon tandem solar cells

Received 00th January 20xx,
Accepted 00th January 20xx

DOI: 10.1039/x0xx00000x

Kong Liu,[ab] Bo Chen,*[bc] Zhengshan J. Yu,[d] Yulin Wu,[a] Zhitao Huang,[a] Xiaohao Jia,[a] Chao Li,[a] Derrek Spronk,[c] Zhijie Wang,[a] Zhanguo Wang,[a] Shengchun Qu,*[a] Zachary C. Holman*[d] and Jinsong Huang*[bc]

Reducing damages caused by sputtering of transparent conductive oxide (TCO) electrodes is critical in achieving highly efficient and stable perovskite/silicon tandem solar cells. Here we study the sputter caused damage to bathocuproine (BCP), which is widely used in highly efficient p-i-n structure single junction perovskite solar cells. While BCP buffer layer protects the underneath layers from damage, itself can be damaged by sputtering of TCOs at a wide range of target-substrate distances, supported by molecular dynamic simulation. More intriguingly, it is observed that TCO easily peeled off after sputtering when the sputtering target is close to substrate. This is ascribed to formation of stress during cooling down process after sputtering due to different thermal expansion coefficients of the layers. Our studies explain why tin oxide ($SnO_2$) made by atomic layer deposition can replace BCP for a much better tandem device performance. $SnO_2$ has high affinity with sputtered TCO electrode to suppress peeling-off issue and has higher bond energy to resist sputter induced damage, thus it allows a wider window of target-substrate distances than BCP during TCO sputtering. Ultimately, we demonstrate an efficient perovskite/silicon monolithic tandem solar cell with efficiency of 26.0% to illustrate the beneficial effects of reduced stress and damage.

## 1. Introduction

The metal halide perovskite/silicon tandem solar cells are promising for achieving efficiency beyond that of single-junction solar cells, potentially resulting in lower levelized cost of electricity.[1-9] In these solar cells, transparent conductive electrodes are required to transmit the incident sunlight. Transparent conductive oxide (TCO) like indium zinc oxide (IZO) have been widely used as top electrodes in semitransparent solar cells and tandem solar cells.[10-13] Magnetron sputtering is the most widely used industrial technique to deposit IZO.[14] However, some challenges may present when IZO sputtering is applied to perovskite top sub-cells. The first one is that the mismatch of thermal expansion coefficients between layers may introduce stress in films, since sputtering process could involve a large temperature change. The second is that high-energy sputtered atoms, ions, electrons, or ultraviolet light produced during sputtering processes may damage perovskite or organic layers in perovskite solar cells by changing their chemical bonding.[15, 16]

The typical single-junction p-i-n structure perovskite solar cells have a structure of ITO/poly(triaryl amine)/perovskite/ETL/BCP/Cu, where ETL is the electron transport layer such as Phenyl-C61-butyric acid methyl ester, Indene $C_{60}$ Bis Adduct (ICBA), $C_{60}$, or a double fullerene layer.[17, 18] The BCP buffer layer is very important for high-performance solar cells, because it reduces charge recombination at the ETL/Cu interface.[19-21] But, as a soft organic material, BCP suffers from damage when the thermal evaporated Cu electrode is replaced with sputtered TCO. Several studies employed perovskite top cells with $SnO_2$, which is deposited by atomic layer deposition (ALD), as buffer layer to reduce sputter damage during TCO deposition.[22-25] However, there is no study yet about the stress in sputtered IZO electrode and corresponding peeling-off issue when the stress is out of the tolerance range. It is unclear yet how sputter process actually damages BCP, and why $SnO_2$ can resist the damage. It is also unknown whether the sputtering process would damage layers underneath BCP, such as $C_{60}$ and perovskite film. Moreover, whether $SnO_2$ can tolerate the sputter induced stress and avoid sputter damage at any sputtering condition need to be investigated as well. To clarify these issues will help us to determine sputtering parameters for TCO of perovskite/silicon tandem solar cells, which is vital for balance between fabrication cost and materials properties.

In this work, we investigate the stress related damage issue induced by sputtering IZO when different buffer layers of BCP and $SnO_2$ are used. We present mechanisms and mitigation approaches for sputter induced stress in perovskite solar cells. Reasons for better performance in the semi-transparent solar cells with $SnO_2$ buffer layer than that with BCP buffer layer is

[a] Key Laboratory of Semiconductor Materials Science, Institute of Semiconductors, Chinese Academy of Sciences, Beijing, 100083, China. E-mail: qsc@semi.ac.cn.
[b] Department of Mechanical and Materials Engineering, University of Nebraska-Lincoln, Lincoln, NE 68588, USA.
[c] Department of Applied Physical Sciences, University of North Carolina, Chapel Hill, NC 27599, USA. E-mail: jhuang@unc.edu, bochen@unc.edu.
[d] School of Electrical, Computer, and Energy Engineering, Arizona State University, Tempe, AZ 85287, USA. E-mail: Zachary.Holman@asu.edu
† Footnotes relating to the title and/or authors should appear here.
Electronic Supplementary Information (ESI) available: [details of any supplementary information available should be included here]. See DOI: 10.1039/x0xx00000x

discussed. Molecular dynamics (MD) simulations are introduced to understand the damage process of sputtered atoms on BCP. Also, the possible peeling-off risk in IZO electrode on $SnO_2$ buffer layer is examined, and the method to overcome it is provided. An efficient perovskite/silicon tandem solar cells is presented to prove the beneficial effect of our strategies.

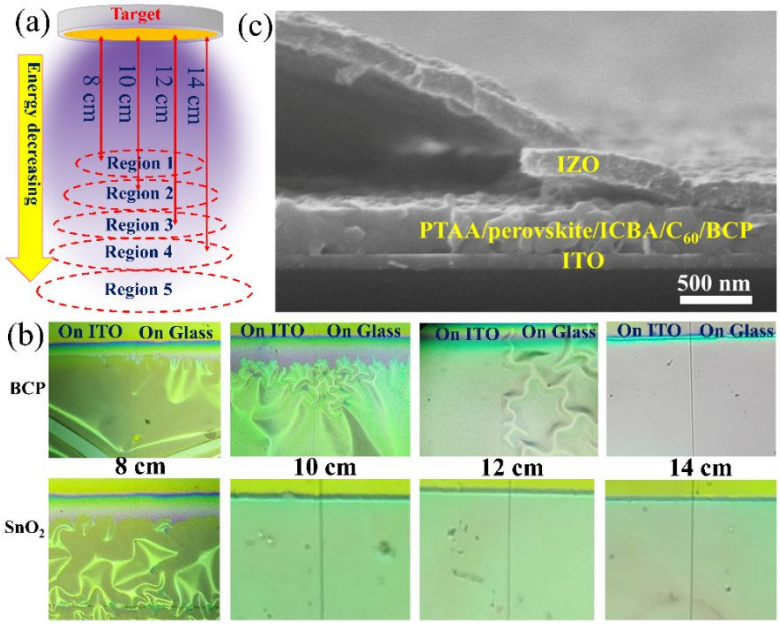


**Fig. 1** (a) Schematic diagram of the IZO sputtering process with different target-substrate distances. (b) Different peeling-off results in IZO electrodes after sputtering at target-substrate distances of 8 cm, 10 cm, 12 cm, and 14 cm with BCP or $SnO_2$ as buffer layer. (c) Cross-section SEM image of a perovskite solar cell with BCP buffer layer and peeled off IZO electrodes deposited at a target-substrate distance of 10 cm.

## 2. Results and discussion

**Peeling-off phenomenon in IZO**

We first observed a peeling-off problem of sputtered IZO electrode for semitransparent perovskite solar cells with BCP and $SnO_2$ buffer layer. The main parameter we tuned in this study was the target-substrate distance, as illustrated in Fig. 1a. Peeling-off of IZO electrode from underneath layers after sputtering on semitransparent perovskite solar cells with BCP buffer layer was observed at a wide range of target-substrate distances from 8 cm to 12 cm; while this peeling-off issue only happened at a short target-substrate distance of 8 cm for solar cells with $SnO_2$ buffer layer, as shown in Fig. 1b and Fig. S1. It was noted that the peeling-off phenomenon didn't occur during the sputtering process but occurred after sputtering during sample cooling down process, which indicates that the change of thermal conditions may be the reason for the phenomenon. The cross-section SEM image in Fig. 1c shows the peeling-off issue caused bad contact between IZO electrode and underneath layer.

**Mechanism for sputter induced stress reduction**

The peeling-off phenomenon of the IZO electrode indicates that there is stress in the sputtered IZO electrode. We speculated that a mismatch of the thermal expansion coefficients between sputtered IZO layer and the underlying layers caused the peeling-off issue. To test this hypothesis, we measured the temperature of sample surface during sputtering at different target-substrate distances with temperature indicators. This experiment revealed that the temperature reached 71 °C, 54 °C and 43 °C when the substrate-target distances were 8 cm, 10 cm and 12 cm, respectively, but the temperature remained below 37 °C when the substrate-target distance increased to 14 cm. It has been reported that the kinetic energy of sputtered atoms can reach 100 eV, which is about 100 times larger than the energies of evaporated particles.[26, 27] This kinetic energy can convert to thermal energy after bombardment with sample. It is noted that the sputtered atoms experience collisions with Ar atoms on their path to the substrate, reducing their kinetic energy. Therefore, the temperature of samples decreases accordingly when they are farther away from the target.

Since the temperature changes with target-substrate distance, the thermal expansion of underlying films shows the same tendency. As illustrated in Fig. 2a, the different thermal expansion coefficients between layers caused peeling-off of IZO layer after sputtering during cooling down process. The thermal expansion coefficients of perovskite and organic layers ($3\times10^{-5}$–$5\times10^{-5}$ $K^{-1}$) are one order of magnitude higher than TCO films and glass substrates ($5\times10^{-6}$–$7\times10^{-6}$ $K^{-1}$). [28-30] When the samples were placed at a target-substrate distance of 8 cm, the soft perovskite and organic films expanded due to elevated temperature during sputtering; when the solar cells cooled to room temperature after sputtering, the perovskite and organic layers contracted more than the IZO film, which caused large stress in the sputtered IZO film. Specifically, tensile stress formed in perovskite/organic layers and compressive stress formed in IZO layer. If the stress was large enough (as calculated in Supporting Information), it would cause severe peeling-off of the IZO electrode, as shown in Fig. 2a and b. At a target-substrate distance of 14 cm, the lower local temperature resulted in less stress and thus mitigated the peeling-off issue for solar cells with BCP buffer layer, as show in Fig. 2c.

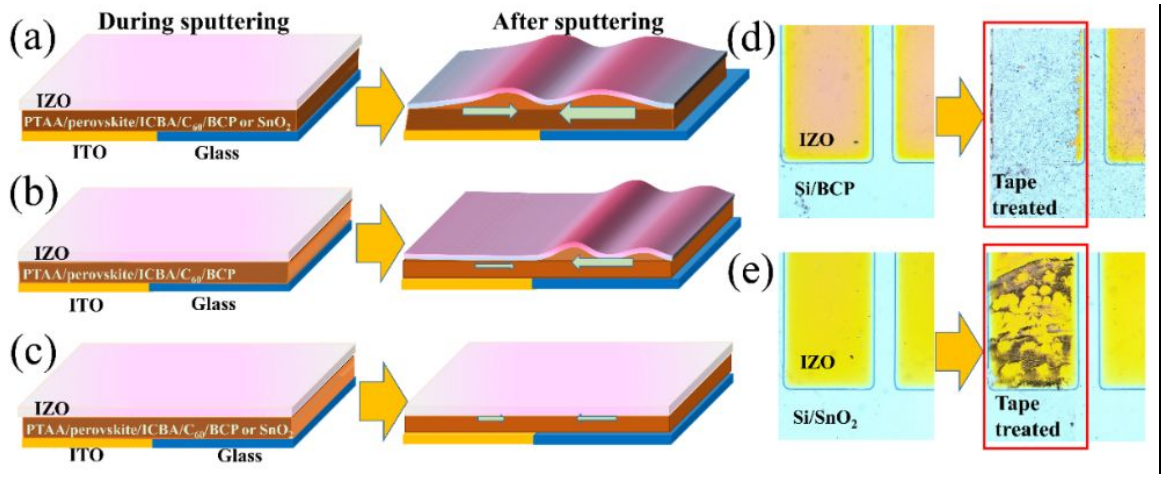


**Fig. 2** Schematic diagram of the formation of IZO peeling-off (a) both on ITO and ITO/glass substrate, and (b) only on glass side. (c) Schematic diagram of the formation of IZO without peeling-off. (d) IZO fingers on BCP film before and after treated by a tape. (e) IZO fingers on $SnO_2$ film before and after treated by a tape.

**Effects of affinity on IZO peeling-off**

We also considered whether the peeling-off of sputtered IZO electrode was due to the stress caused by the insertion of particles like indium, zinc, or oxygen during sputtering. If this was the case, the peeling-off phenomena would occur during the sputtering process, rather than during device cool down process after sputtering, which is opposite to the experimental observation. Moreover, we found that the substrate property also affected the peeling-off location. The substrates we used to make the devices were glass substrates with only half area coating with ITO bottom electrode. When we sputtered the IZO top electrode for BCP-devices at a target-substrate distance of 12 cm, the peeling-off phenomenon of the IZO electrode only occurred at location without ITO bottom electrode, as shown in Fig. 1b and Fig. S1c. If the stress induced by insertion of sputtered particles dominated the peeling-off phenomenon, there would be no difference of stress and peeling-off phenomenon in locations with and without ITO bottom electrode. Therefore, we believe this difference is due to different stress release on different substrates during cooling down process. In our previous study,[31] we found that the perovskite film coated on glass side generally showed less strain than the perovskite film coated on ITO/glass side, which was ascribed to the different bonding strength between the perovskites and substrates due to different roughness of ITO and glass. Less affinity or bonding of perovskites to the smooth and nonwetting glass substrates allow the perovskite films on glass release strain much easier than on rough ITO. For the same reason, when temperature cooled down after sputtering, the perovskite film on glass could have larger contraction than the film on ITO substrates, which created larger stress between perovskite film and sputtered IZO electrode at location of bare glass and caused peeling-off, as shown in Fig. 2b.

Since no IZO peeling-off was observed in solar cells based on $SnO_2$ buffer layer when IZO was deposited at a target-substrate distance of 10 cm or longer, we speculated that better affinity between $SnO_2$ with adjacent layers was formed. This is because that $SnO_2$ and IZO are both metal oxide, which will benefit formation of strong bonding between them. While BCP is organic molecular, the contact between IZO and BCP is based on Van der Waals force. To verify this, we deposited IZO fingers onto BCP and $SnO_2$ films on silicon substrates and then tried to tear IZO fingers with tape. Fig. 2d and e show the results of tearing IZO fingers on BCP and $SnO_2$ films. It was found that the IZO on BCP can be peeled off easily while IZO on $SnO_2$ was very firm, which revealed the better affinity between IZO and $SnO_2$ than that between IZO and BCP. The cross-section SEM image of perovskite solar cell with $SnO_2$ buffer layer in Fig. S2 also shows good contact between $SnO_2$ and IZO layers.

We also studied whether using ALD-$SnO_2$ can ultimately solve the IZO peeling-off issue by reducing the substrate temperature to an unpractically low value of -5 °C. We found that IZO still peeled off in the $SnO_2$ samples when target-substrate distance was 10 cm, as show in Fig. S3. No change was observed for the samples when target-substrate distances were 12 cm or 14 cm. It indicates that an appropriately large target-substrate distance is still needed for $SnO_2$-devices.

**Influences of sputter induced molecular level damage in BCP**

Despite that a large target-substrate distance could generate less stress in the sputtered IZO to avoid peeling-off issue of TCO electrode itself, sputtering of IZO could still damage other layers. Perovskite, fullerene, and BCP in the perovskite sub-cells are all soft materials that have either low cohesive energy between the atoms or low bond dissociation energy between the molecules.[16, 32] The bombardment of them by high-energy particles might cause atomic or molecular level damage which will reduce their electronic properties. In order to evaluate the influence of sputter damage on electronic properties, we fabricated perovskite solar cells with the structure of ITO/PTAA/perovskite/ICBA/$C_{60}$/BCP/IZO/Cu by sputtering a 10-nm-thick IZO electrode at a target-substrate distance of 14 cm and then thermal evaporating 80-nm-thick Cu, as shown in Fig. 3a. In this design, thermal evaporated Cu electrode enhanced the conductivity of the IZO electrode, where the thin IZO electrode was introduced to evaluate the sputter damage. Fig. 3b shows that the IZO/Cu-device exhibited a very low fill factor (*FF*) and an obvious S-shape in the *J-V* curve, while the control device that only had thermal evaporated Cu electrode

performed much well. It indicates that the sputtering process still caused damages to the other layers.[15] If the Cu electrode was also deposited by sputtering rather than by thermal evaporation, a similar *J-V* curve with low *FF* and S-shape was also found (Fig. S4), which further proves that the worse device performance was caused by sputter damage, rather than the new interfaces introduced by IZO. This suggests that even though a larger sputtering distance can avoid the stress issue, it cannot completely eliminate the sputter caused molecular level damage in BCP buffer layer.

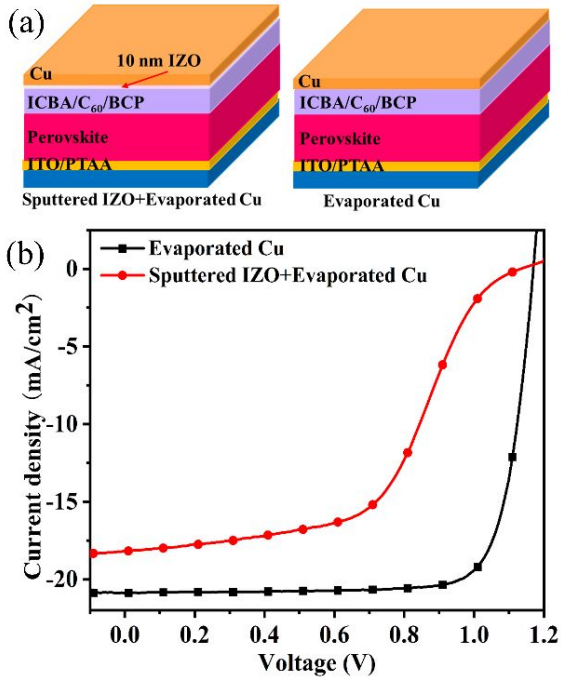


**Fig. 3** (a) Schematics of perovskite solar cells with and without a 10-nm-thick IZO film under the Cu electrode. (b) *J-V* characteristics of the perovskite solar cells with Cu and IZO/Cu electrodes.

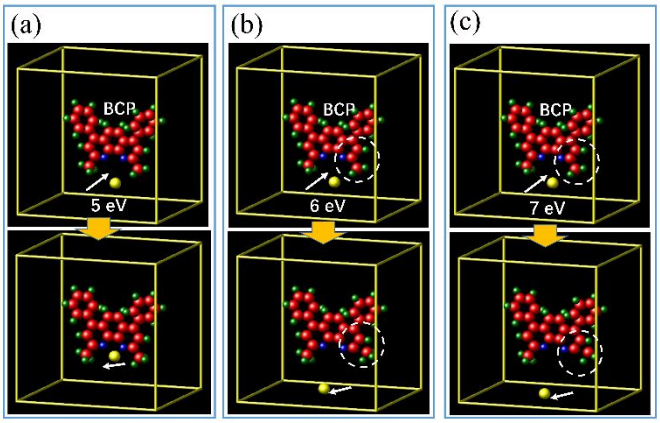


**Fig. 4** MD simulations of collisions between sputtered indium atoms and BCP molecules. The incident energy of the indium atoms is set to (a) 5 eV, (b) 6 eV, and (c) 7 eV. The first row shows the system before collision; the second row shows the system after collision. The circles in (b) and (c) denote differences in position and distance of atoms, which can illustrate the damage in BCP.

**MD simulation on molecular level damage in BCP**

In order to reveal how BCP was damaged, we performed MD simulations on the collision process between sputtered indium atoms and BCP molecules. The indium atom was selected because it has the highest mass compared to zinc, oxygen, and argon atoms. According to the law of conservation of momentum, indium atoms will loss less kinetic energy per collision with, e.g., Ar atoms than other sputtered atoms, and will thus arrive at the substrate with the most energy. The energies of indium atoms in the range of 1 eV to 10 eV were simulated. We also varied the incidence of the indium atoms to hit different atoms in BCP, and we found that the C-C bond connecting the methyl group was the most easily broken. Therefore, the damage was most likely to occur at the C-C bond in BCP during sputtering, and we focused our simulation at this position. Fig. 4a-c shows simulated collisions processes with three different indium energies near the damage threshold. For indium atoms with energy of 5 eV, the methyl group did not change its position and the distance of adjacent two carbon atoms kept the same after collision (Fig. 4a). For indium atoms with energy of 6 eV and 7 eV, the methyl group was bombarded away from its original position and the distance of adjacent two carbon atoms was changed (Fig. 4b and c). It reveals that the C-C bond in BCP can break by indium atoms with energy of 6 eV and higher. This energy threshold indicates the reason why sputter damage could occur in BCP but not in $SnO_2$. Because the Sn-O bond energy in $SnO_2$ films is about 528 kJ $mol^{-1}$ (5.47 eV),[33] which is much higher than the C-C bond energy (3.59 eV) in BCP molecules. This means that it requires a higher energy for sputtered atoms to break down $SnO_2$.

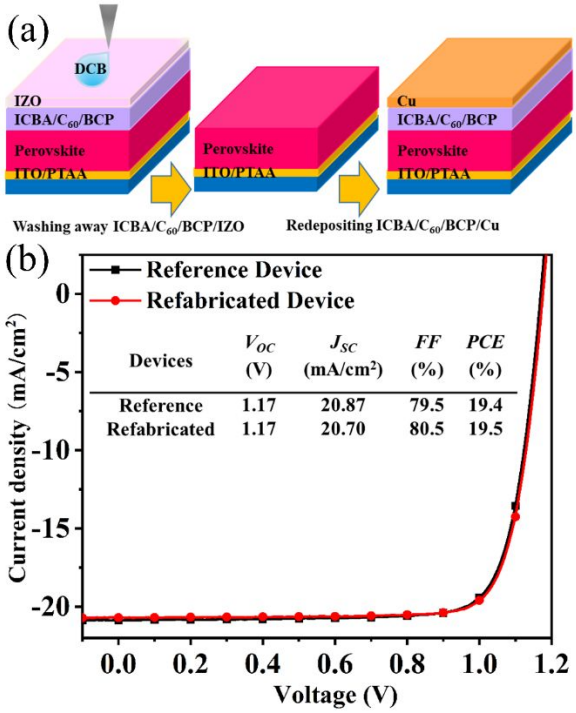


**Fig. 5** (a) Procedure for refabricating a perovskite solar cell by replacing ICBA/$C_{60}$/BCP/IZO with new layers of ICBA/$C_{60}$/BCP/Cu. (b) *J-V* characteristics of the perovskite solar cell after refabrication, compared to a control device with an original Cu electrode.

**Investigation on damage of underlying layers**

Since the device efficiency reduction can come from damage of any layer in the perovskite solar cells, we studied whether the sputter damage penetrated into other layers underneath BCP for solar cells with BCP or $SnO_2$ buffer layers. We fabricated a perovskite solar cell with sputtered IZO electrodes, and then we washed off the ICBA/$C_{60}$/BCP/IZO layers by 1,2-dichlorobenzene (DCB), as shown in Fig. 5a. We next deposited ICBA/$C_{60}$/BCP/Cu on the perovskite again. Fig. 5b shows the *J-V* results of the re-fabricated device and the reference device with evaporated Cu electrodes on BCP directly. The original perovskite solar cell with sputtered IZO electrode here has S-curve similar as *J-V* curve of solar cell with IZO/Cu in Fig. 3b. However, we can see that the re-fabricated device does not show any performance degradation compared to reference device, which has the same *J-V* curve of solar cell with evaporated Cu in Fig. 3b. This reveals that the sputtering process did not damage the underlying perovskite layer. For further verification, we performed MD simulations on collisions between indium atoms and $C_{60}$ molecules with different atom energies. Fig. S5 shows that bond rupture in $C_{60}$ molecule happens only when the energy of the sputtered indium exceeds 200 eV, which is much higher than the initial energy of sputtered atoms from the target. For indium atoms with energy lower than 200 eV, no obvious changes were found in $C_{60}$ structure. Besides, the indium atoms were reflected back by the carbon atoms. Therefore, it is unlikely that the sputtered atoms can cause damage to the layers underneath the $C_{60}$ layer and we only need to consider the sputter damage issues in the BCP layer.

**Achieving efficient perovskite/silicon tandem solar cell**

Since the substrate-target distance of 14 cm is still not large enough to avoid the damage of BCP by high energy particles during sputtering process, we attempted to further increase the substrate-target distance. However, both the conductivity and transmittance of IZO films become worse when the target-substrate distance was increased to beyond 14 cm, as shown in Fig. S6. This is because sputtered atoms with too low energy generally results in porous and rough morphology of IZO film.[34, 35] $SnO_2$ is an excellent buffer layer to allow a wide range of target-substrate distance to resist the sputter damage as well as to tolerate the sputter induced stress, which enable fabrication of efficient semi-transparent perovskite solar cells and tandem solar cells.

We fabricated a complete perovskite/silicon tandem solar cell with $SnO_2$ buffer layer and IZO electrode deposited at a target-substrate distance of 12 cm to check the beneficial effects of elimination of sputter damage and peeling-off issue. Fig. 6a shows the structure of the tandem device. The corresponding cross-section SEM image of perovskite sub-cell in Fig. 6b also shows good contact between each layers without peeling-off issue. No peeling-off of IZO electrode was observed after the tandem device cooled to -5 °C to enlarge the residual stress, which indicates strong adhesion between IZO electrode and underneath layers. Thanks both to the sputter protection provided by $SnO_2$ and the optimized IZO sputtering process, the tandem solar cell reached a *PCE* of 26.0% (Fig. 6c). There was no obvious *PCE* degradation for the un-encapsulated tandem device under illumination at maximum power point at ~55 °C in air for 120 min (Fig. S7). The external quantum efficiency (EQE) of the tandem device showed current match between sub-cells (Fig. S8). The absence of hysteresis and high *FF* indicate that the charge recombination and interfacial barrier introduced by sputter damage and stress have been suppressed due to reduction of sputter damage using the optimized sputtering conditions and $SnO_2$ buffer layers.

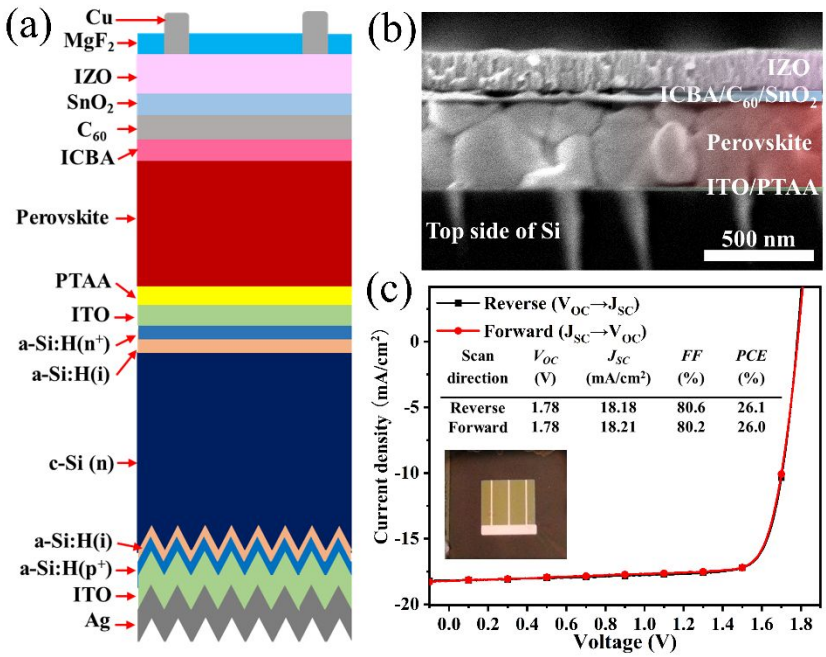


**Fig. 6** (a) Schematic of a perovskite/silicon tandem solar cell with a $SnO_2$ buffer layer. (b) Cross-section SEM image of perovskite top sub-cell of the tandem solar cell. (c) *J-V* characteristics of the perovskite/silicon tandem solar cell under forward and reverse scans. Inset in (c): Image of the perovskite/silicon monolithic tandem solar cell.

## Conclusions

In summary, we investigated the sputtering process of IZO electrodes on the perovskite top sub-cell of perovskite/silicon tandem solar cells with focus on the mechanism for peeling-off and sputter damage. The peeling-off of sputtered IZO electrode was avoided by increasing the target-substrate distance to 14 cm for BCP buffer layer and 10 cm for $SnO_2$ buffer layer, but sputter damage to the BCP buffer layer persisted at these distances. MD simulations showed that energetic sputtered atoms with a kinetic energy of greater than 6 eV can break C-C bonds in BCP molecules. It was proved that buffer layer is the key to address the sputter damage issue, because the sputter damage did not penetrate into the underlying layers. When utilizing $SnO_2$ as the buffer layer, strong affinity between sputtered IZO and buffer layer was formed and thus peeling-off issue was suppressed. A high *PCE* of 26.0% was obtained in perovskite/silicon tandem solar cell when these strategies were applied. This work demonstrates that the combination of appropriate target-substrate distance and a robust buffer layer is a solution to suppress the stress in IZO film and avoid the bond rupture in the buffer layer.

## Author Contributions

J. H., Z. H., B. C., and S. Q. conceived the idea. K. L. conducted sputtering deposition and molecular dynamics simulation. K. L. and B. C. fabricated the wide-bandgap solar cells and perovskite/silicon tandem cells. Z. Y. fabricated the silicon bottom cells. Y. W. fabricated films and conducted SEM test. Z. H. and X. J. performed calculations. D. S. and C. L. carried out ALD. Z. W. and Z. W. analysed optical and electrical properties of TCO. K. L., B. C., and J. H. wrote the paper, and all authors reviewed the paper.

## Conflicts of interest

There are no conflicts to declare.

## Acknowledgements

The information, data, or work presented herein is funded by U.S. Department of Energy's Office of Energy Efficiency and Renewable Energy (EERE) under Solar Energy Technologies Office (SETO) (Agreement Number DE-EE0008749) and by the UNC Research Opportunities Initiative through the Center of Hybrid Materials Enabled Electronic Technology. Prof. K. Liu also acknowledges the support from Youth Innovation Promotion Association, Chinese Academy of Sciences (No. 2020114).

## References

1 K. A. Bush, C. D. Bailie, Y. Chen, A. R. Bowring, W. Wang, W. Ma, T. Leijtens, F. Moghadam and M. D. McGehee, *Adv. Mater.*, 2016, **28**, 3937-3943.

2 H. R. Tan, A. Jain, O. Voznyy, X. Z. Lan, F. P. G. de Arquer, J. Z. Fan, R. Quintero-Bermudez, M. J. Yuan, B. Zhang, Y. C. Zhao, F. J. Fan, P. C. Li, L. N. Quan, Y. B. Zhao, Z. H. Lu, Z. Y. Yang, S. Hoogland and E. H. Sargent, *Science*, 2017, **355**, 722-726.

3 G. E. Eperon, T. Leijtens, K. A. Bush, R. Prasanna, T. Green, J. T. W. Wang, D. P. McMeekin, G. Volonakis, R. L. Milot, R. May, A. Palmstrom, D. J. Slotcavage, R. A. Belisle, J. B. Patel, E. S. Parrott, R. J. Sutton, W. Ma, F. Moghadam, B. Conings, A. Babayigit, H. G. Boyen, S. Bent, F. Giustino, L. M. Herz, M. B. Johnston, M. D. McGehee and H. J. Snaith, *Science*, 2016, **354**, 861-865.

4 M. B. Upama, M. A. Mahmud, H. M. Yi, N. K. Elumalai, G. Conibeer, D. Wang, C. Xu and A. Uddin, *Org. Electron.*, 2019, **65**, 401-411.

5 T. Leijtens, K. A. Bush, R. Prasanna and M. D. McGehee, *Nat. Energy*, 2018, **3**, 828-838.

6 Y. G. Rong, Y. Hu, A. Y. Mei, H. R. Tan, M. I. Saidaminov, S. I. Seok, M. D. McGehee, E. H. Sargent and H. W. Han, *Science*, 2018, **361**, eaat8235.

7 Z. S. Yu, M. Leilaeioun and Z. Holman, *Nat. Energy*, 2016, **1**, 16137.

8 Z. S. J. Yu, J. V. Carpenter and Z. C. Holman, *Nat. Energy*, 2018, **3**, 747-753.

9 L. K. Zheng, J. L. Wang, Y. M. Xuan, M. Y. Yan, X. X. Yu, Y. Peng and Y. B. Cheng, *J. Mater. Chem. A*, 2019, **7**, 26479-26489.

10 K. A. Bush, A. F. Palmstrom, Z. S. J. Yu, M. Boccard, R. Cheacharoen, J. P. Mailoa, D. P. McMeekin, R. L. Z. Hoye, C. D. Bailie, T. Leijtens, I. M. Peters, M. C. Minichetti, N. Rolston, R. Prasanna, S. Sofia, D. Harwood, W. Ma, F. Moghadam, H. J. Snaith, T. Buonassisi, Z. C. Holman, S. F. Bent and M. D. McGehee, *Nat. Energy*, 2017, **2**, 17009.

11 F. Sahli, J. Werner, B. A. Kamino, M. Brauninger, R. Monnard, B. Paviet-Salomon, L. Barraud, L. Ding, J. J. D. Leon, D. Sacchetto, G. Cattaneo, M. Despeisse, M. Boccard, S. Nicolay, Q. Jeangros, B. Niesen and C. Ballif, *Nat. Mater.*, 2018, **17**, 820-826.

12 M. Jost, E. Kohnen, A. B. Morales-Vilches, B. Lipovsek, K. Jager, B. Macco, A. Al-Ashouri, J. Krc, L. Korte, B. Rech, R. Schlatmann, M. Topic, B. Stannowski and S. Albrecht, *Energ. Environ. Sci.*, 2018, **11**, 3511-3523.

13 B. Chen, Z. Yu, K. Liu, X. Zheng, Y. Liu, J. Shi, D. Spronk, P. N. Rudd, Z. Holman and J. Huang, *Joule*, 2019, **3**, 177-190.

14 T. Minami, *Thin Solid Films*, 2008, **516**, 5822-5828.

15 H. Kanda, A. Uzum, A. K. Baranwal, T. A. N. Peiris, T. Umeyama, H. Imahori, H. Segawa, T. Miyasaka and S. Ito, *J. Phys. Chem. C*, 2016, **120**, 28441-28447.

16 H. Lei, M. H. Wang, Y. Hoshi, T. Uchida, S. Kobayashi and Y. Sawada, *Appl. Surf. Sci.*, 2013, **285**, 389-394.

17 X. P. Zheng, Y. Hou, C. X. Bao, J. Yin, F. L. Yuan, Z. R. Huang, K. P. Song, J. K. Liu, J. Troughton, N. Gasparini, C. Zhou, Y. B. Lin, D. J. Xue, B. Chen, A. K. Johnston, N. Wei, M. N. Hedhili, M. Y. Wei, A. Y. Alsalloum, P. Maity, B. Turedi, C. Yang, D. Baran, T. D. Anthopoulos, Y. Han, Z. H. Lu, O. F. Mohammed, F. Gao, E. H. Sargent and O. M. Bakr, *Nat. Energy*, 2020, **5**, 131-140.

18 D. Y. Luo, W. Q. Yang, Z. P. Wang, A. Sadhanala, Q. Hu, R. Su, R. Shivanna, G. F. Trindade, J. F. Watts, Z. J. Xu, T. H. Liu, K. Chen, F. J. Ye, P. Wu, L. C. Zhao, J. Wu, Y. G. Tu, Y. F. Zhang, X. Y. Yang, W. Zhang, R. H. Friend, Q. H. Gong, H. J. Snaith and R. Zhu, *Science*, 2018, **360**, 1442-1446.

19 J. Y. Jeng, Y. F. Chiang, M. H. Lee, S. R. Peng, T. F. Guo, P. Chen and T. C. Wen, *Adv. Mater.*, 2013, **25**, 3727-3732.

20 N. Shibayama, H. Kanda, T. W. Kim, H. Segawa and S. Ito, *APL Mater.*, 2019, **7**, 031117.

21 R. Xia, Y. B. Xu, B. B. Chen, H. Kanda, M. Franckevicius, R. Gegevicius, S. B. Wang, Y. F. Chen, D. M. Chen, J. N. Ding, N. Y. Yuan, Y. Zhao, C. Roldan-Carmona, X. D. Zhang, P. J. Dyson and M. K. Nazeeruddin, *J. Mater. Chem. A*, 2021, **9**, 21939-21947.
22 A. Al-Ashouri, E. Kohnen, B. Li, A. Magomedov, H. Hempel, P. Caprioglio, J. A. Marquez, A. B. M. Vilches, E. Kasparavicius, J. A. Smith, N. Phung, D. Menzel, M. Grischek, L. Kegelmann, D. Skroblin, C. Gollwitzer, T. Malinauskas, M. Jost, G. Matic, B. Rech, R. Schlatmann, M. Topic, L. Korte, A. Abate, B. Stannowski, D. Neher, M. Stolterfoht, T. Unold, V. Getautis and S. Albrecht, *Science*, 2020, **370**, 1300-1309.
23 Y. Hou, E. Aydin, M. De Bastiani, C. Xiao, F. H. Isikgor, D.-J. Xue, B. Chen, H. Chen, B. Bahrami, A. H. Chowdhury, A. Johnston, S.-W. Baek, Z. Huang, M. Wei, Y. Dong, J. Troughton, R. Jalmood, A. J. Mirabelli, T. G. Allen, E. Van Kerschaver, M. I. Saidaminov, D. Baran, Q. Qiao, K. Zhu, S. De Wolf and E. H. Sargent, *Science*, 2020, **367**, 1135-1140.
24 J. Xu, C. C. Boyd, Z. J. Yu, A. F. Palmstrom, D. J. Witter, B. W. Larson, R. M. France, J. Werner, S. P. Harvey, E. J. Wolf, W. Weigand, S. Manzoor, M. F. A. M. van Hest, J. J. Berry, J. M. Luther, Z. C. Holman and M. D. McGehee, *Science*, 2020, **367**, 1097-1104.
25 H. R. Liu, Z. L. Chen, H. B. Wang, F. H. Ye, J. J. Ma, X. L. Zheng, P. B. Gui, L. B. Xiong, J. Wen and G. J. Fang, *J. Mater. Chem. A*, 2019, **7**, 10636-10643.
26 T. Motohiro and Y. Taga, *Thin Solid Films*, 1984, **112**, 161-173.
27 P. F. Carcia, R. S. McLean, M. H. Reilly, Z. G. Li, L. J. Pillione and R. F. Messier, *J. Vac. Sci. Technol. A*, 2003, **21**, 745-751.
28 Y. Rakita, S. R. Cohen, N. K. Kedem, G. Hodes and D. Cahen, *MRS Commun.*, 2015, **5**, 623-629.
29 M. N. Saleh and G. Lubineau, *Sol. Energ. Mat. Sol. C*, 2014, **130**, 199-207.
30 A. T. Pugachev, N. P. Churakova, N. I. Gorbenko, K. Saadli and E. S. Syrkin, *J. Exp. Theor. Phys.*, 1998, **87**, 1014-1018.
31 J. J. Zhao, Y. H. Deng, H. T. Wei, X. P. Zheng, Z. H. Yu, Y. C. Shao, J. E. Shield and J. S. Huang, *Sci. Adv.*, 2017, **3**, eaao5616.
32 E. Salonen, K. Nordlund, J. Keinonen and C. H. Wu, *Europhys. Lett.*, 2000, **52**, 504-510.
33 M. Fondell, M. Gorgoi, M. Boman and A. Lindblad, *J. Electron Spectrosc.*, 2014, **195**, 195-199.
34 J. A. Thornton, *J. Vac. Sci. Technol.*, 1974, **11**, 666-670.
35 J. H. E. Cartwright, B. Escribano, O. Piro, C. I. Sainz-Diaz, P. A. Sanchez and T. Sintes, *AIP Conf. Proc.*, 2008, **982**, 696-701.